Indirect exchange interaction between magnetic adatoms in monolayer MoS_2

F. Parhizgar, H. Rostami, and Reza Asgari*
School of Physics, Institute for Research in Fundamental Sciences (IPM), Tehran 19395-5531, Iran
(Received 10 December 2012; published 4 March 2013)

We study the Ruderman-Kittle-Kasuya-Yosida (RKKY) interaction in a monolayer MoS_2. We show that the rotation of the itinerant electron spin due to the spin-orbit coupling causes a twisted interaction between two magnetic adatoms, which consists of different RKKY coupling terms: the Heisenberg, Dzyaloshinsky-Moriya, and Ising interactions. We find that the interaction terms are very sensitive to the Fermi energy values and change dramatically from doped to undoped systems. A finite doping causes all parts of the interaction to oscillate with the distance of two magnetic impurities R, and the interaction behaves like R^{-2} for a long distance between two localized spins. We explore a beating pattern of oscillations of the RKKY interaction that occurs for the doped system.

DOI: 10.1103/PhysRevB.87.125401 PACS number(s): 75.30.Hx, 75.10.Lp, 73.63.−b

I. INTRODUCTION

Two-dimensional (2D) materials can be mostly exfoliated into individual thin layers from stacks of strongly bonded layers with weak interlayer interaction. A famous example is graphene[1] and its analogs such as boron nitride.[2] The 2D exfoliate versions of transition metal dichalcogenides[3] exhibit properties that are complementary to and distinct from those in graphene. MoS_2 (the polytype, 2H-MoS_2, has trigonal prismatic coordination) is a hexagonal crystal layered structure with a covalently bonded S-Mo-S hexagonal quasi-two-dimensional network, which does not have inversion symmetry, packed by weak van der Waals interactions. The monolayer of MoS_2 has provided a new material with a peculiar structure for the charge and the spin interactions.[4] There is a transition from an indirect band gap of 1.3 eV in a bulk structure to a direct band gap of 1.8 eV in the monolayer structure.[5] This direct band gap opens the possibility of many optoelectronic applications.[5] The electronic structure of MoS_2 also enables valley polarization[6–9] since both the conduction and valence band edges have two energy-degenerate valleys at the corners of the first Brillouin zone and valley selective circular dichroism arising from its symmetry.

Ruderman-Kittle-Kasuya-Yosida (RKKY) interaction is an indirect interaction between the nuclei of transition metals or magnetic impurities, mediated by the conduction electrons.[10–12] This interaction is directly related to the spin susceptibility of the host metal. Rudermann and Kittel first suggested[10] that the spin oscillatory interaction in metals could provide a long-range interaction between nuclear spins and explored the effective magnetic interaction between nuclei of transition metals and thus described the reason for the broadening of spin resonance line diagram. Due to the fact that the RKKY interaction originates from the exchange coupling between the impurity moments and the spin of itinerant electrons in the bulk of the system, a spin splitting owing to spin-orbit coupling is expected to influence directly this interaction. Since the two inequivalent valleys in the monolayer MoS_2 are separated in the Brillouin zone by a large momentum, in the case of the absence of short-range interactions, intervalley scattering[13] should be negligible and thus the valley index becomes a new quantum number. Therefore manipulating the valley quantum number can produce new physical effects.

In the monolayer MoS_2, the highest energy valence bands and the lowest energy conduction bands, at the K and K' valleys in momentum space, are mainly of molybdenum d-orbital character, and spin-orbit interaction splits[14] the valence bands by $2\lambda \sim 150$ meV leading to a spin polarization of the valence band. A minimal effective band model Hamiltonian of MoS_2 is found by Xiao *et al.*[14] with parameters based on first-principles calculations. To first order in momenta, the first part of Hamiltonian describes the dynamics of massive Dirac fermions, which is studied by the graphene committees. It is commonly known that the RKKY interaction in massless graphene is quite different[15–17] from that of a Schrödinger 2D electron liquid. The second part of the Hamiltonian illustrates the spin-orbit interaction, which leads to coupled spin and valley physics in the monolayer MoS_2. The RKKY interaction usually yields a Heisenberg coupling referring to a parallel or an antiparallel coupling of localized spins. If the spin of conduction electrons precesses, it can possibly produce a noncollinear Dzyaloshinsky-Moriaya (DM) coupling of localized spins. We, thus, use this model Hamiltonian to calculate the exchange interaction between localized spins on the MoS_2 and show that, in particular, the combination of the spin valley with a massive Dirac-like spectrum can mediate a much richer collective behavior of magnetic adatoms.

The RKKY interaction in 2D electron gas in the presence of a Rashba spin-orbit coupling has been studied by Imamura *et al.*[18] and they showed that the rotation of the spin of conduction electrons causes a twisted RKKY interaction, which consists of three different terms, the Heisenberg, DM, and Ising interactions. Moreover, the RKKY interaction between localized magnetic moments in a disordered 2D electron gas with both Rashba and Dresselhaus spin-orbit couplings has been studied.[19] The disorder-averaged susceptibility leads to a twisted exchange interaction suppressed exponentially with distance, whereas the second-order correlations, which determine the fluctuations of the RKKY energy, decay with the same power law as in the clean case.

In this work, we calculate the RKKY interaction mediated by spin-orbit coupled massive Dirac fermions in a monolayer MoS_2 using the Green's function method. We show that the interaction consists of three terms without the Rashba or Dresselhaus interaction and show, in particular, that the

interaction behaves like R^{-2} for a long distance between two localized spins. The DM coupling leads to a rotation of the spinors of magnetic moments with respect to each other. In addition, a beating pattern for the interaction, in the cases where the monolayer MoS_2 system is doped, is obtained. As we mentioned before, the model Hamiltonian can be reduced to a massive graphene by discarding the spin-orbit coupling. Besides the R^{-3} dependence of the interaction for undoped massless graphene, we find that the interaction decays like R^{-2} for a massive and doped graphene. However, for a massive and undoped graphene, the interaction decays rapidly in a good agreement with those results obtained in Ref. 20.

The paper is organized as follows. In Sec. II, we introduce the formalism that will be used in calculating the RKKY interaction from the Green's function. In Sec. III, we present our analytic and numeric results for the coupling strengths of the RKKY interaction in both undoped and doped monolayer MoS_2 sheets. Section IV contains discussions and a brief summary of our main results.

II. METHOD AND THEORY

The Hamiltonian for a single-layer MoS_2 including two magnetic impurities can be written as $\hat{\mathcal{H}} = \hat{\mathcal{H}}_0 + \hat{\mathcal{H}}_{\rm int}$, where $\hat{\mathcal{H}}_0$ is the noninteracting Hamiltonian for the single-layer MoS_2 and $\hat{\mathcal{H}}_{\rm int}$ is the interaction term between impurities and spin of conduction electrons. In the monolayer MoS_2, the highest energy valence bands and the lowest energy conduction bands, at the K and K' valleys in momentum space, are mainly of molybdenum d-orbital character and spin-orbit interaction splits[14] the valence bands by $2\lambda \sim 150$ meV leading to a spin polarization of the valence band. Figure 1 shows the band dispersion of monolayer MoS_2 in which the spin splitting in

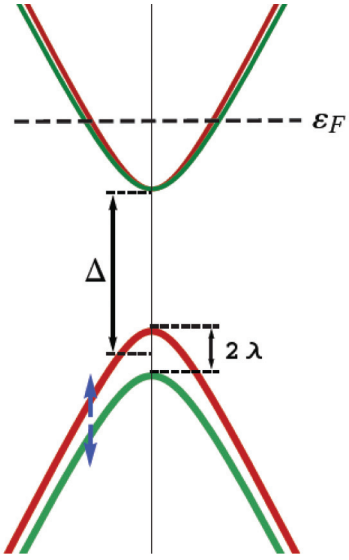

FIG. 1. (Color online) Schematic picture of the dispersion relation in momentum space at valley K. The valence and conduction bands are separated by a large direct band gap Δ and there is a large spin-orbit coupling λ leading to a spin polarization of the valence band (spin up $\uparrow$ and spin down $\downarrow$). The dispersion relation is given by $E(k) = \frac{\lambda}{2}\tau s_z \pm \sqrt{(atk)^2 + (\Delta/2 - \lambda\tau s_z/2)^2}$.

conduction band is negligible, however, a spin splitting in the valence band leads to a spin shift.

The Hamiltonian for MoS_2 in a continuum model at K and K' points is written as[14]

$$\hat{\mathcal{H}}_0^\tau = at(\tau k_x\hat{\sigma}_x + k_y\hat{\sigma}_y) + \frac{\Delta}{2}\hat{\sigma}_z - \lambda\tau\frac{\hat{\sigma}_z - 1}{2}\hat{s}_z, \qquad (1)$$

where the index τ is ± 1 at valley K or K', Δ is the direct band gap, λ is the spin-orbit coupling constant, a is the lattice parameter, and t is the hoping integral. $\hat{\sigma}$'s are the Pauli matrices written in pseudospinor $\psi^\dagger = (\Phi_c^\dagger, \Phi_v^{\tau\dagger})$, where c and v denote the conduction and valence bands, respectively, and finally $\hat{s}_z$ is the Pauli matrix for the z component of spin.

Particulary, the noninteracting Hamiltonian in the spinor basis, $\psi^\dagger = (c_{k,\uparrow}^\dagger, v_{k,\uparrow}^\dagger, c_{k,\downarrow}^\dagger, v_{k,\downarrow}^\dagger)$, can be written as

$$\hat{\mathcal{H}}_0^\tau = \begin{pmatrix} \Delta/2 & at\tau k e^{-i\tau\theta'} & 0 & 0 \\ at\tau k e^{i\tau\theta'} & -\Delta/2 + \lambda\tau & 0 & 0 \\ 0 & 0 & \Delta/2 & at\tau k e^{-i\tau\theta'} \\ 0 & 0 & at\tau k e^{i\tau\theta'} & -\Delta/2 - \lambda\tau \end{pmatrix}, \qquad (2)$$

where $\theta' = \tan^{-1}(k_y/k_x)$. Here the system in question incorporates two localized magnetic moments whose interaction is mediated through a large spin-orbit coupled electron gas. The contact interaction between the spin of itinerant electrons and two magnetic impurities with magnetic moments $\mathbf{I_1}$ and $\mathbf{I_2}$, located, respectively, at $\mathbf{R}_1$ and $\mathbf{R}_2$, is given by

$$\hat{\mathcal{H}}_{\rm int} = J_c \sum_{j=1,2} \mathbf{I}_j \cdot \mathbf{s}(\mathbf{R}_j), \qquad (3)$$

where J_c is the coupling constant between conduction electrons and impurity (we set $\hbar = 1$ from now on), $\mathbf{s}(\mathbf{r}) = \frac{1}{2}\sum_i \delta(\mathbf{r}_i - \mathbf{r})\sigma_i$ is the spin density operator with $\mathbf{r}_i$ and σ_i being the position and vector of spin operators of ith electron, respectively.

The RKKY interaction, which arises from the quantum effects, is obtained by using a second-order perturbation,[10–12,18] which reads as

$$\hat{\mathcal{H}}_{\rm RKKY} = J_c^2 \sum_{i,j} I_1^i \chi_{ij}(\mathbf{R},\mathbf{R}') I_2^j, \qquad (4)$$

where $\chi_{ij}(\mathbf{R},\mathbf{R}')$ is the spin susceptibility in real space given by $\chi_{ij}(\mathbf{R},\mathbf{R}') = \sum_{\alpha\in(c,v)} \chi_{ij}^{\alpha\alpha}(\mathbf{R},\mathbf{R}')$, in which

$$\chi_{ij}^{\alpha\beta}(\mathbf{R},\mathbf{R}') = \frac{-1}{2\pi}{\rm Tr}\Big\{ \int_{-\infty}^{\varepsilon_F} d\varepsilon \Im m[\sigma_i G^{\alpha\beta}(\mathbf{R},\mathbf{R}',\varepsilon) \times \sigma_j G^{\beta\alpha}(\mathbf{R}',\mathbf{R},\varepsilon)]\Big\}. \qquad (5)$$

Here, α and β denote pseudospin degree of freedom, ε_F is the Fermi energy, the trace is taken over the spin degree of freedom, and σ is the Pauli spin matrix. $G^{\alpha\beta}(\mathbf{R},\mathbf{R}';\varepsilon)$ is a 2×2 matrix of the single-particle retarded Green's functions in spin space. In order to calculate the interaction Hamiltonian of Eq. (4), the form of the electronic single-particle Green's function, $G(\mathbf{R},\underline{\mathrm{R}}';\varepsilon) = \langle\mathbf{R}|(\varepsilon + i0^+ - \hat{\mathcal{H}}_0)^{-1}|\mathbf{R}'\rangle$ is needed. To calculate the retarded Green's function in real space,

its Fourier components in momentum space might be first obtained:

$$G(k,\varepsilon)=\begin{pmatrix} \frac{\varepsilon+\Delta/2-\lambda\tau}{(\varepsilon-\Delta/2)(\varepsilon+\Delta/2-\lambda\tau)-a^2t^2k^2} & \frac{at\tau ke^{-i\tau\theta'}}{(\varepsilon-\Delta/2)(\varepsilon+\Delta/2-\lambda\tau)-a^2t^2k^2} & 0 & 0 \\ \frac{at\tau ke^{i\tau\theta'}}{(\varepsilon-\Delta/2)(\varepsilon+\Delta/2-\lambda\tau)-a^2t^2k^2} & \frac{\varepsilon-\Delta/2}{(\varepsilon-\Delta/2)(\varepsilon+\Delta/2-\lambda\tau)-a^2t^2k^2} & 0 & 0 \\ 0 & 0 & \frac{\varepsilon+\Delta/2+\lambda\tau}{(\varepsilon-\Delta/2)(\varepsilon+\Delta/2+\lambda\tau)-a^2t^2k^2} & \frac{at\tau ke^{-i\tau\theta'}}{(\varepsilon-\Delta/2)(\varepsilon+\Delta/2+\lambda\tau)-a^2t^2k^2} \\ 0 & 0 & \frac{at\tau ke^{i\tau\theta'}}{(\varepsilon-\Delta/2)(\varepsilon+\Delta/2+\lambda\tau)-a^2t^2k^2} & \frac{\varepsilon-\Delta/2}{(\varepsilon-\Delta/2)(\varepsilon+\Delta/2+\lambda\tau)-a^2t^2k^2} \end{pmatrix}. \quad (6)$$

Generally, the energy dispersion of the noninteracting system can be obtained by the pole of the Green's function and it reads as $E(k)=\frac{\lambda}{2}\tau s_z \pm \sqrt{(atk)^2+(\Delta/2-\lambda\tau s_z/2)^2}$. The retarded Green's functions are diagonal in the spin space, $G_{cc}(q,\varepsilon)=\begin{pmatrix}\frac{\alpha_-}{\beta_--q^2} & 0\\ 0 & \frac{\alpha_+}{\beta_+-q^2}\end{pmatrix}$ and $G_{vv}(q,\varepsilon)=\begin{pmatrix}\frac{\alpha}{\beta_--q^2} & 0\\ 0 & \frac{\alpha}{\beta_+-q^2}\end{pmatrix}$, where $\alpha_\pm=(\varepsilon+\Delta/2\pm\lambda)/(at)^2$, $\alpha=(\varepsilon-\Delta/2)/(at)^2$, and $\beta_\pm=(\varepsilon-\Delta/2)(\varepsilon+\Delta/2\pm\lambda)/(at)^2$. Taking the Fourier transform of the matrices, we thus find the real space Green's function matrix

$$G_{cc}(\mathbf{R},0,\varepsilon)=\frac{1}{(2\pi)^2}\int d^2q\{e^{i\mathbf{K}\cdot\mathbf{R}}e^{i\mathbf{q}\cdot\mathbf{R}}G_{cc}[q(K)\varepsilon] + e^{i\mathbf{K}'\cdot\mathbf{R}}e^{i\mathbf{q}\cdot\mathbf{R}}G_{cc}[q(K'),\varepsilon]\}, \quad (7)$$

where $q(K)$ or $q(K')$ is the wave vector near the Dirac point K or K', respectively. The integral can be simply calculated and it thus reads as

$$G_{cc}(\mathbf{R},0,\varepsilon)=\begin{pmatrix} e^{i\mathbf{K}\cdot\mathbf{R}}g_{c-}+e^{i\mathbf{K}'\cdot\mathbf{R}}g_{c+} & 0 \\ 0 & e^{i\mathbf{K}\cdot\mathbf{R}}g_{c+}+e^{i\mathbf{K}'\cdot\mathbf{R}}g_{c-}\end{pmatrix}, \quad (8)$$

where $g_{c\pm}(|\mathbf{R}|)=-\alpha_\pm K_0(\sqrt{-\beta_\pm}|\mathbf{R}|)/(2\pi)$, in which $K_0(x)$ is the modified Bessel function of the second kind. We can follow conveniently the same procedure discussed above to obtain $G^0_{cc}(0,\mathbf{R},\varepsilon)=G^0_{cc}(-\mathbf{R},0,\varepsilon)$. Moreover, the obtained retarded Green's function $G^0_{vv}(\mathbf{R},0,\varepsilon)$ is the same as for the channel (cc), only $g_{c\pm}(|\mathbf{R}|)$ is replaced by $g_{v\pm}(|\mathbf{R}|)=-\alpha K_0(\sqrt{-\beta_\pm}|\mathbf{R}|)/(2\pi)$.

By inserting the retarded Green's functions in Eq. (4) and taking the trace over the spin degree of matrices, the RKKY Hamiltonian simplifies to

$$\hat{\mathcal{H}}_{\mathrm{RKKY}}=J_c^2\chi_{xx}(I_{1x}I_{2x}+I_{1y}I_{2y})+J_c^2[\chi_{xy}(I_1\times I_2)_z + \chi_{zz}I_{1z}I_{2z}], \quad (9)$$

which indicates that the RKKY interaction consists of three different terms: the Heisenberg like $I_1\cdot I_2$, Ising $I_{1z}I_{2z}$, and Dzyaloshinsky-Moriya $(I_1\times I_2)_z$ terms. Accordingly, the RKKY Hamiltonian can be written as

$$\hat{\mathcal{H}}_{\mathrm{RKKY}}=J_H\hat{H}_H+J_I\hat{H}_I+J_{\mathrm{DM}}\hat{H}_{\mathrm{DM}}, \quad (10)$$

where $J_i=-\frac{J_c^2}{2\pi}\int_{-\infty}^{\varepsilon_F}d\varepsilon\Im m\eta_i$ and

$$\eta_H=\sum_{a\in(c,v)}4g_{a+}g_{a-}+2\left(g_{a+}^2+g_{a-}^2\right)\cos[(\mathbf{K}-\mathbf{K}')\cdot\mathbf{R}],$$
$$\eta_I=\sum_{a\in(c,v)}2(g_{a+}-g_{a-})^2\{1-\cos[(\mathbf{K}-\mathbf{K}')\cdot\mathbf{R}]\}, \quad (11)$$
$$\eta_{\mathrm{DM}}=\sum_{a\in(c,v)}-2\left(g_{a+}^2-g_{a-}^2\right)\sin[(\mathbf{K}-\mathbf{K}')\cdot\mathbf{R}].$$

The resulting RKKY interaction consists of three quite different interactions. The Heisenberg and Ising interactions favor a collinear alignment of localized spins. On the contrary, the DM coupling favors a noncollinear alignment of localized spins. The same form of Hamiltonian has been obtained in 2D electron gas in the presence of Rashba spin-orbit coupling[18] and in the topological insulators, in which magnetic impurities exhibit a frustrated RKKY interaction with two possible phases of ordered ferromagnetic phase and a disordered spin glass phase.[21] Importantly, the existence of J_{DM} in those systems is a consequence of spin changing term, however, in the monolayer MoS_2 system, the DM coupling is a consequence of the spin-orbit coupling and the existence of two inequivalent valleys separated by $(\mathbf{K}-\mathbf{K}')$. Consequently, the DM term results in noncollinearity of two spinors interacting to each other. In addition, all coupling terms in the Hamiltonian for the monolayer MoS_2 system depend on the direction between the magnetic impurities.

III. NUMERICAL RESULTS

In this section, we present in the following our main results for the numerical evaluation of the RKKY exchange coupling in massive Dirac fermions by analyzing the above calculated integrals of J_H, J_{DM}, and J_I. We set[14] $a=3.193$ Å, $\Delta=1.66$ eV, $2\lambda=150$ meV, and $t=1.1$ eV in all our results presented in this section. We also consider two valleys at $K=(2\pi)(1,\sqrt{3})/(3\sqrt{3}a)$ and $K'=(2\pi)(-1,\sqrt{3})/(3\sqrt{3}a)$.

At finite value of the Fermi energy, in electron or hole doped cases, a more complicated behavior of the RKKY coupling can occur. In this case, the behavior of all J_i interactions is determined by a superposition of two modified Bessel functions with two different periods determined by arguments in $\beta_\pm$. As a result, we observe that for doped MoS_2, the oscillations of J_i exhibit a beating pattern. Figure 2(a) shows this beating behavior of integral J_H [scaled by $J_c^2/(2\pi)^3a^2$] as a function of the impurity distance along the x direction (zigzag direction) for a Fermi energy that intersects the conduction band at $\varepsilon_{\mathrm{F}}=\Delta/2+\lambda$. Figures 2(b) and 2(c) show a similar behavior for integrals J_{DM} and J_I, respectively, as a function of distance along x direction. Our numerical results show that all coupling interactions decay as R^{-2} at finite Fermi energy and in a long-range regime, $J_I>J_H>J_{\mathrm{DM}}$. As it is obvious from Eq. (11), the couplings J_{DM} and J_I vanish when $\lambda\to 0$. Therefore the existence of DM and Ising interactions is a consequence of spin-orbit coupling without having Rashba or Dresselhaus interactions. Besides, since $g_{c\pm}$ are coupled to the Dirac points differently, as diagonal elements in Eq. (8), the DM coupling is nonzero as long as one has the spin-orbit coupling together with two inequivalent valleys. It should be

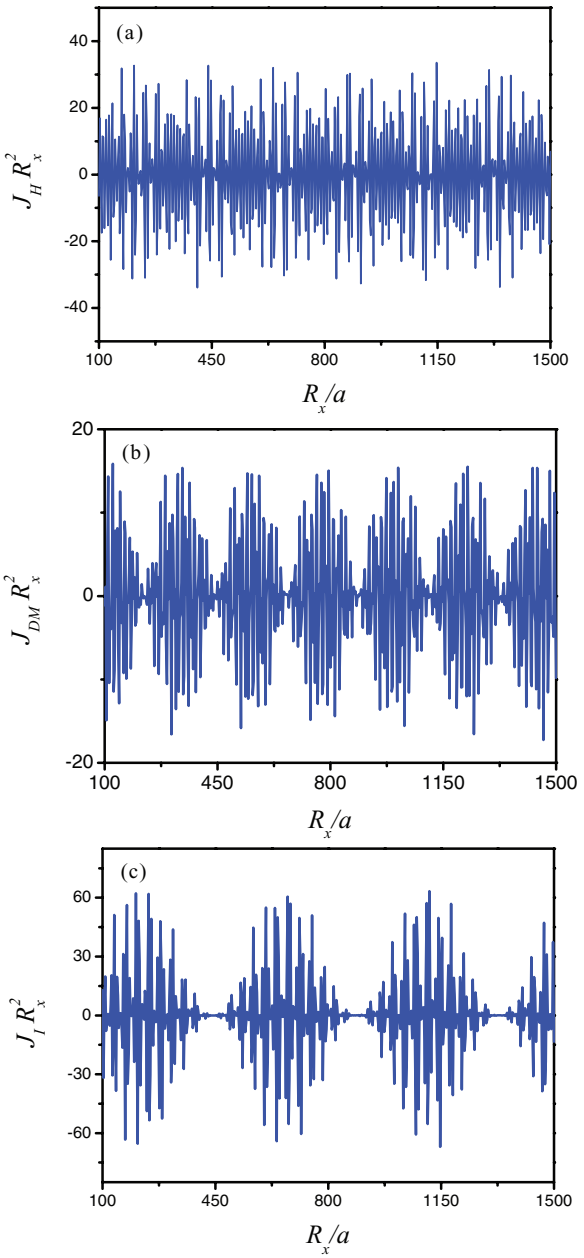

FIG. 2. (Color online) Long-range behavior of RKKY interaction terms, J_i for $i = H$, DM, and I, times R_x^2 scaled by $J_c^2/(2\pi)^3 a^2$ as a function of the impurity distance along the x direction for a Fermi energy that intersects the conduction band at $\varepsilon_F = \Delta/2 + \lambda$. The behavior of all J_i interactions is determined by a superposition of two modified Bessel functions (see the text) with two different periods determined by arguments in $\beta_\pm$. Moreover, the RKKY interaction terms in doped MoS_2 decay as R^{-2} at long-range distance.

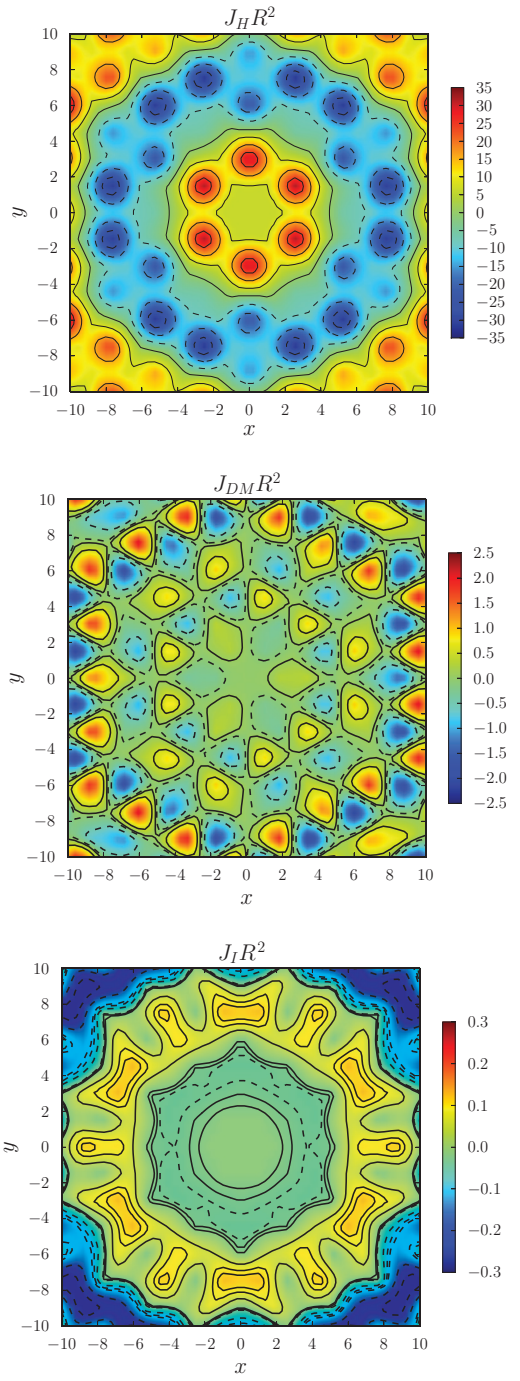

FIG. 3. (Color online) Short-range contour plot of RKKY interaction terms, J_i for $i = H$, DM, or I, scaled by $J_c^2/(2\pi)^3 a^2$ as a function of the impurity distance in (x, y) plane scaled by a for Fermi energy $\varepsilon_F = \Delta/2 + \lambda$. One of the spins is fixed at the origin and another can be located on lattice points. Solid lines denote boundaries with positive values of the interaction term, while dashed lines refer to its negative values. The results show clearly the threefold symmetry.

noticed that there are some locations along x direction for which $J_{DM} \gg J_H$, since they have two different periods and this leads to a strong rotation even at long distance.

Notice that in the MoS_2 system, the RKKY interaction is direction dependent, which is in contrast to the results obtained in the topological insulators or 2D electron gas systems. Since the RKKY interaction is a weak one and decays as R^{-2} in the MoS_2 system, it would be good to look at its short-range behavior. Figure 3 shows the angle dependence of J_i in a contour plot scheme for a short distance and for $\varepsilon_F = \Delta/2 + \lambda$. Here, the system is electron doped and we assume that one of the spins is fixed at origin and another can be located on lattice points. Close to the impurity positions, the effective interaction comes mainly from the J_H interaction and it is ferromagnetic, it becomes antiferromagnetic at a

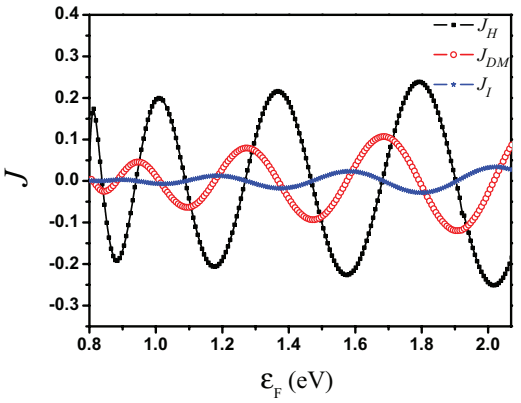

FIG. 4. (Color online) RKKY interaction terms, J_i for $i = H$, DM, or I, scaled by $J_c^2/(2\pi)^3a^2$ as a function of doping electron energy in units of eV at $\mathbf{R} = (4\sqrt{3}a,0)$. Since there is a phase difference between J_i's, for certain values of the Fermi energy, there are situations in which $J_{\rm DM} > J_H$.

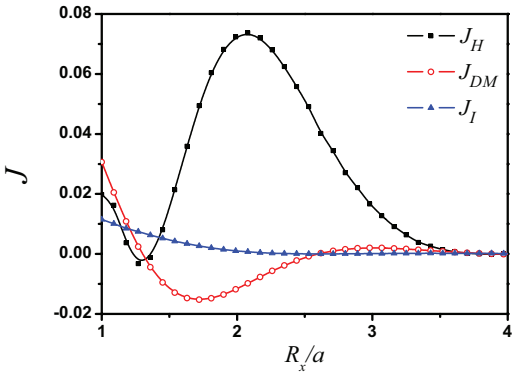

FIG. 5. (Color online) Short-range behavior of RKKY interaction terms, J_i for $i = H$, DM, or I, scaled by $J_c^2/(2\pi)^3a^2$ as a function of the impurity distance along the x direction for an undoped monolayer MoS_2 system where $\varepsilon_F = 0$. J_i coupling interactions tend to zero quickly and, moreover, J_H and J_I are mostly negative and the interaction is antiferromagnetic.

distance comparable to $\sim 2a$. As expected, the amplitude of oscillations decreases with increasing distance between the local moment impurities. Moreover, the threefold symmetry of the band structure is reflected in the susceptibility and thus in the magnetic interactions. The threefold symmetry is clear in this figure.

For a situation where the Fermi energy has an intersection with the valence bands (hole-doped case), the RKKY interaction terms are exhibiting oscillatory behavior structures, however, the magnitude of the interactions is different from those obtained for the case of the electron-doped system. An intriguing feature of the RKKY interaction is its dependence on the Fermi energy values. The Fermi energy dependence of the RKKY interaction for a fixed distance between two impurities, $\mathbf{R} = (4\sqrt{3}a,0)$, is shown in Fig. 4, in which the Fermi energy always intersects the conduction band. The interaction amplitudes increase by increasing the Fermi energy and the period of the oscillations remains constant. It is expected that the values of $J_{\rm DM}$ and J_I, in the short range, are small since the contribution of the spin splitting in the conduction band is negligible. Owing to a phase difference between J_i's, for certain values of the Fermi energy, there are situations in which $J_{\rm DM} > J_H$. Interestingly enough, for certain values of the Fermi energy and the distance between two magnetic impurities, $J_{\rm DM} > J_H$, and this leads to a strong rotation between spins of impurities. Accordingly, by designing an arbitrary artificial lattice with magnetic impurities (e.g., triangular or square with an arbitrary lattice constant) and by properly adjusting the distance $\mathbf{R}$ using scanning tunneling microscope techniques, we will be able to control each coupling term in the RKKY interaction and therefore the monolayer MoS_2 would be a quite good platform to exhibit different spin lattices and interactions.

On the other hand, for an undoped MoS_2 system, the response of electron decreases exponentially and therefore the RKKY interaction terms fall off rapidly. The same behavior occurs in topological insulators when the Fermi energy lies in the gap.[22] Figure 5 shows the RKKY interaction terms for an undoped monolayer MoS_2. Those interactions decay fast, which shows that the interactions are rather short ranged[23] and decrease to zero quickly. Moreover, J_H and J_I are mostly positive, which shows that the coupling between the moments remains antiferromagnetic-like for all Rs.

In the monolayer MoS_2, there are two valence bands, which are separated out by the spin-orbit interaction and, furthermore, each band has a different s_z value (see Fig. 1). The top valence band starts at $\varepsilon = -\Delta/2 + \lambda$, whereas the other band starts at $\varepsilon = -\Delta/2 - \lambda$. Figure 6 shows the behavior of the RKKY interaction terms with respect to the Fermi energy in the region where the valence band is occupied. For the case where $\varepsilon_F < -\Delta/2 - \lambda$, an important result is obtained. First of all, the RKKY interaction terms exhibit oscillatory structures and their amplitudes are suppressed by increasing the Fermi energy. This behavior occurs till the Fermi energy reaches to the top valence band illustrated by a shadowed layer in Fig. 6 and afterwards the RKKY interaction terms decay rapidly. The reason for such a decay comes from the fact that the one-spin channel, for such Fermi energy value, is blocked and therefore the magnetic spin can not be coupled to the host electrons. In other words, in this

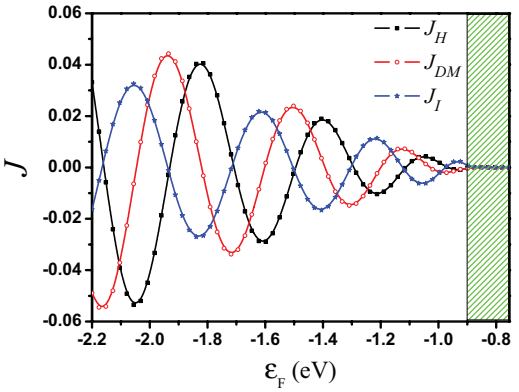

FIG. 6. (Color online) RKKY interaction terms, J_i for $i = H$, DM, or I, scaled by $J_c^2/(2\pi)^3a^2$ as a function of doping hole energy, where $\varepsilon_F < -\Delta/2 - \lambda$ for $\mathbf{R} = (4\sqrt{3}a,0)$. The RKKY interaction terms oscillate and their amplitudes are suppressed by increasing the Fermi energy level until it reaches the top of the valence band, illustrated by a shadowed layer.

case, the spin susceptibility of the system tends to zero since the spin relaxation time of the monolayer MoS_2 is quite long[14] when the intervalley scattering is ignored.

A. Twisted angle: a classical picture

As discussed before, the DM term causes a twisted interaction between two magnetic adatoms. In order to calculate the equilibrium angle of the interaction, we simplify the RKKY interaction Hamiltonian in the spherical coordinate as

$$\hat{\mathcal{H}}_{\mathrm{RKKY}} = I_1 I_2 (J_H + J_I)\cos\theta_1 \cos\theta_2 + I_1 I_2 \sin\theta_1 \sin\theta_2 (J_H \cos\phi + J_{\mathrm{DM}} \sin\phi), \quad (12)$$

where $\theta_{1(2)}$ denotes the angle between the spin along the z direction and $\phi = \phi_2 - \phi_1$. The equilibrium conditions, $\partial\hat{\mathcal{H}}_{\mathrm{RKKY}}/\partial\theta_1 = 0$, $\partial\hat{\mathcal{H}}_{\mathrm{RKKY}}/\partial\theta_2 = 0$, and $\partial\hat{\mathcal{H}}_{\mathrm{RKKY}}/\partial\phi = 0$, lead to the following equations:

$$\begin{aligned} &-(J_H + J_I)\cos\theta_2 \sin\theta_1 \\ &\quad + \sin\theta_2 \cos\theta_1 (J_H \cos\phi + J_{\mathrm{DM}} \sin\phi) = 0, \\ &-(J_H + J_I)\cos\theta_1 \sin\theta_2 \\ &\quad + \sin\theta_1 \cos\theta_2 (J_H \cos\phi + J_{\mathrm{DM}} \sin\phi) = 0, \\ &\sin\theta_1 \sin\theta_2 (-J_H \sin\phi + J_{\mathrm{DM}} \cos\phi) = 0. \end{aligned} \quad (13)$$

There are solutions for Eq. (13) at the boundary of the square $(\theta_1 - \theta_2)$ plane that are conveniently given by $\pi(1,0)$, $\pi(0,1)$, $\pi(0,0)$, and $\pi(1,1)$. For those solutions at the boundaries, the only possible configurations of the two magnetic impurities are ferromagnetic- or antiferromagnetic-like ones. Moreover, there is just one extremum point at $\theta_1 = \theta_2 = \theta = \pi/2$ between $\theta = 0$ and π. The states of the system are described by maximum, minimum, or saddle behaviors of the extremum. An intriguing case can occur for the situation when the extremum is a local minimum. In this case, the equilibrium condition leads to the case when the moments lie in the sample's plane with an angle $\phi = \tan^{-1}(J_{\mathrm{DM}}/J_H)$ between two magnetic moments.

In order to describe the extremum behavior at point $\theta = \pi/2$, we do need to evaluate the positive definite condition of the Hessian matrix of Eq. (12) throughout a neighbor of $\theta = \pi/2$, which is the second derivative of the RKKY Hamiltonian with respect to free variables,[24] and it yields

$$D_1 = -\mathrm{sign}(J_H)\sqrt{J_H^2 + J_{\mathrm{DM}}^2},$$
$$D_2 = J_{\mathrm{DM}}^2 - J_I(2J_H + J_I).$$

For a case when $D_1 > 0$ and $D_2 > 0$, the critical point $\theta = \pi/2$ is a local minimum of the system that we would like to explore. However, for the situation in which $D_1 < 0$ and $D_2 > 0$, the critical point is a local maximum of the system. A saddle point, on the other hand, is described by the condition that $D_1 > 0$ and $D_2 < 0$ or $D_1 < 0$ and $D_2 < 0$. In the last two cases, the equilibrium state of the system is obeyed by the boundary solutions, which are given by ferromagnetic- or antiferromagnetic-like configurations.

Figure 7 shows the sign of D_1 and D_2 as a function of the Fermi energy in the conduction band when the distance vector between impurities is $\mathbf{R} = (4\sqrt{3}a, 0)$. A saddle point, minimum, and maximum regions take place by increasing the Fermi energy from the bottom of the conduction band. The inset shows the angle ϕ between moments for the middle region in which both D_1 and D_2 are positive and $\theta = \pi/2$.

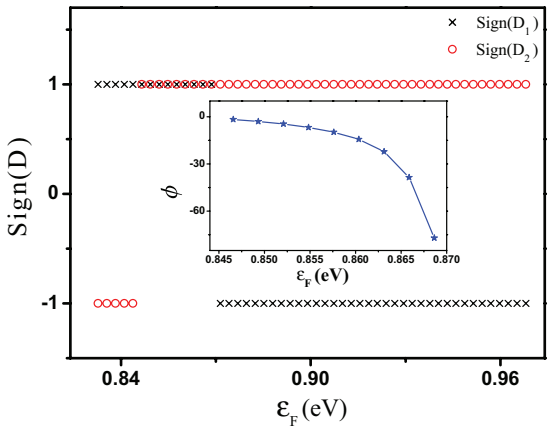

FIG. 7. (Color online) Sign of D_1 and D_2 as a function of the Fermi energy in the conduction band for $\mathbf{R} = (4\sqrt{3}a, 0)$. The inset shows the angle $\phi = \tan^{-1}(J_{\mathrm{DM}}/J_H)$ between two magnetic moments when D_1 and D_2 are both positive.

IV. SUMMARY AND CONCLUSIONS

We study the influence of spin-orbit coupling on the RKKY interaction in a monolayer MoS_2 system. We use the Green's function method in the continuum model. We show that the rotation of the itinerant spin causes a twisted interaction between two magnetic adatoms, which consists of different RKKY coupling terms, the Heisenberg, Dzyaloshinsky-Moriya, and Ising interactions. We explore different scenarios of two magnetic moments in terms of the different RKKY coupling values. We also find that the interaction terms are very sensitive to the Fermi energy values and change dramatically from doped to undoped systems. For the undoped system, we find a short-range interaction between the moments in the most probable antiferromagnetic-like structure. The dependence of the interaction on the distance R between two local magnetic moments is found to be R^{-2} in a doped monolayer MoS_2 sheet. We found that for a dilute electron doping, the Dzyaloshinsky-Moriya interaction can be larger than the Heisenberg interaction for certain values of R. A beating pattern of oscillations of the RKKY interaction, which occurs for the doped system, is discussed.

We conclude that the monolayer MoS_2 is a quite good platform to explore different types of spin Hamiltonian. The interaction terms in the single-layer MoS_2 are quite similar to those terms appearing in the topological insulator system,[22] however, the interaction terms here are direction dependent, whereas in the topological insulators, the interactions are only distance dependent.

ACKNOWLEDGMENT

This work was partially supported by IPM grant.

*asgari@ipm.ir

[1]K. S. Novoselov, A. K. Geim, S. V. Morozov, D. Jiang, Y. Zhang, S. V. Dubonos, I. V. Grigorieva, and A. A. Firsov, Science **306**, 666 (2004).
[2]C. R. Dean, A. F. Young, I. Meric, C. Lee, L. Wang, S. Sorgenfrei, K. Watanabe, T. Taniguchi, P. Kim, K. L. Shepard, and J. Hone, Nat. Nanotechnology **5**, 722 (2010).
[3]L. F. Mattheis, Phys. Rev. B **8**, 3719 (1973).
[4]Q. H. Wang, K. Kalantar-Zadeh, A. Kis, J. N. Colemn, and M. S. Strano, Nat. Nanotechnology **7**, 699 (2012).
[5]A. Kuc, N. Zibouche, and T. Heine, Phys. Rev. B **83**, 245213 (2011).
[6]K. F. Mak, K. He, J. Shan, and T. F. Heinz, Nat. Nanotechnology **7**, 494 (2012).
[7]H. Zeng, J. Dai, W. Yao, D. Xiao, and X. Cui, Nat. Nanotechnology **7**, 490 (2012).
[8]T. Cao, G. Wang, W. Han, H. Ye, C. Zhu, J. Shi, Q. Niu, P. Tan, E. Wang, B. Liu, and J. Feng, Nature Commun. **3**, 887 (2012).
[9]A. Splendiani, L. Sun, Y. Zhang, T. Li, J. Kim, C. Chim, G. Galli, and Feng Wang, Nano Lett. **10**, 1271 (2010).
[10]M. A. Ruderman and C. Kittel, Phys. Rev. **96**, 99 (1954).
[11]T. Kasuya, Prog. Theor. Phys. **16**, 45 (1956).
[12]K. Yosida, Phys. Rev. **106**, 893 (1957).
[13]Hai-Zhou Lu, Wang Yao, Di Xiao, and Shun-Qing Shen, Phys. Rev. Lett. **110**, 016806 (2013).
[14]D. Xiao, G. B. Liu, W. Feng, X. Xu, and W. Yao, Phys. Rev. Lett. **108**, 196802 (2012).
[15]M. A. H. Vozmediano, M. P. López-Sancho, T. Stauber, and F. Guinea, Phys. Rev. B **72**, 155121 (2005); D. A. Abanin, A. V. Shytov, and L. S. Levitov, Phys. Rev. Lett. **105**, 086802 (2010); A. M. Black-Schaffer, Phys. Rev. B **82**, 073409 (2010); **81**, 205416 (2010); S. R. Power, F. S. Guimaráes, A. T. Costa, R. B. Muniz, and M. S. Ferreira, *ibid.* **84**, 195411 (2012); H. Lee, E. R. Mucciolo, G. Bouzerar, and S. Kettemann, *ibid.* **86**, 205427 (2012).
[16]M. Sherafati and S. Satpathy, Phys. Rev. B **83**, 165425 (2011); **84**, 125416 (2011).
[17]F. Parhizgar, R. Asgari, S. H. Abedpour, and M. Zareyan, arXiv:1211.2013.
[18]H. Imamura, P. Bruno, and Y. Utsumi, Phys. Rev. B **69**, 121303(R) (2004).
[19]S. Chesi and D. Loss, Phys. Rev. B **82**, 165303 (2010).
[20]V. K. Dugaev, V. I. Litvinov, and J. Barnas, Phys. Rev. B **74**, 224438 (2006).
[21]D. A. Abanian and D. A. Pesin, Phys. Rev. Lett. **106**, 136802 (2011).
[22]Jia-Ji Zhu, Dao-Xin Yao, Shou-Cheng Zhang, and Kai Chang, Phys. Rev. Lett. **106**, 097201 (2011).
[23]N. Bloembergen and T. J. Rowland, Phys. Rev. **97**, 1679 (1955).
[24]R. A. Adams, *Calculus, A Complete Course* (Addison-Wesley, Toronto, 2003).